GUIDED CIRCUMFERENTIAL WAVES IN LAYERED POROELASTIC CYLINDERS

S.A. SHAH[*]
Department of Mathematics
Deccan College of Engineering and Technology
Hyderabad–500 001 (T.S) INDIA
E-mail: ahmed_shah67@yahoo.com

G. APSAR
Department of Mechanical Engineering
Deccan College of Engineering and Technology
Hyderabad–500 001 (T.S), INDIA

The present paper investigates the propagation of time harmonic circumferential waves in a two-dimensional hollow poroelastic cylinder with an inner shaft (shaft-bearing assembly). The hollow poroelastic cylinder and inner shaft are assumed to be infinite in axial direction. The outer surface of the cylinder is stress free and at the interface, between the inner shaft and the outer cylinder, it is assumed to be free sliding and the interfacial shear stresses are zero, also the normal stress and radial displacements are continuous. The frequency equation of guided circumferential waves for a permeable and an impermeable surface is obtained. When the angular wave number vanish the frequency equation of guided circumferential waves for a permeable and an impermeable surface degenerates and the dilatational and shear waves are uncoupled. Shear waves are independent of the nature of surface. The frequency equation of a permeable and an impermeable surface for bore-piston assembly is obtained as a particular case of the model under consideration when the outer radius of the hollow poroelastic cylinder tends to infinity. Results of previous studies are obtained as a particular case of the present study. Non-dimensional frequency as a function of wave number is presented graphically for two types of models and discussed. Numerical results show that, in general, the first modes are linear for permeable and impermeable surfaces and the frequency of a permeable surface is more than that of an impermeable surface.

Key words: Biot's theory, poroelastic layered cylinder, circumferential waves, shaft-bearing assembly, bore-piston assembly, permeable surface, impermeable surface, wave number, frequency.

1. Introduction

Most of components in engineering usually consist of cylindrical structures composed of at least an inner cylinder and an outer cylinder. Study of fatigue cracks in cylindrical components is important, because due to the application of a load, crack formation follows. These fatigue cracks generally form at the interface between the two layers and they spread in a radial direction. Detection of such radial cracks is important to avoid a severe mechanical failure. A guided wave propagates in the direction of the layer, behaving as a standing wave through the thickness of the layer. Guided waves are commonly used to examine simple structures such as beams and plates and layered cylinders. One such example is given by Nagy *et al* [1], who suggested that radial fatigue cracks in weep holes in airframes may be detected by using guided waves propagating along the circumferential direction of the hole. Christine Valle *et al* [2] investigated the guided circumferential waves in layered cylinders and showed that the waves are non dispersive at high frequency or high wave number. Tajuddin and Shah [3, 4] studied the circumferential waves and torsional vibrations of

---

[*] To whom correspondence should be addressed

hollow poroelastic cylinders in the presence of dissipation and found that the phase velocity is non-dispersive in the case of circumferential waves. Whittier and Jones [5] studied axially symmetric vibrations in a two-layered cylinder. Guided circumferential waves in a circular annulus are studied by Liu and Qu [6]. Malla Reddy and Tajuddin [7] studied the plane-strain vibrations of thick-walled hollow poroelastic cylinders. Towfighi *et al.* [8] discussed the wave propagation in a circumferential direction in anisotropic cylindrical curved plates. Shah [9] presented the solutions for flexural wave propagation in coated poroelastic cylinders where the rule of mixtures is used to understand the dispersion phenomenon in a coated cylinder knowing the frequency equations for the cases of homogeneous poroelastic cylinders made of coating and core poroelastic materials separately.
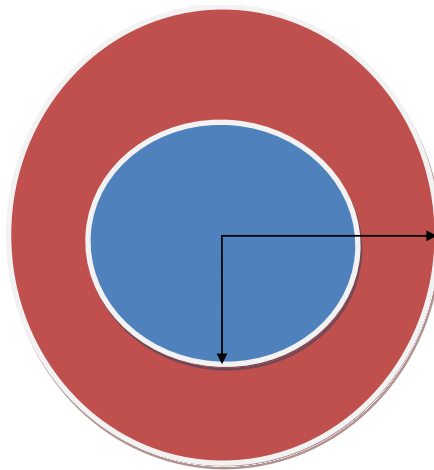

Fig.1. Cross-section of shaft-bearing assembly.

In this paper, guided circumferential waves are studied for the purpose of detecting the radial fatigue cracks in a shaft-bearing assembly that is, a layered poroelastic cylinder. The frequency equation obtained helps in understanding the radial fatigue cracks. For this purpose, it is necessary to understand the behavior of wave propagation in a layered poroelastic cylinder. Time harmonic guided wave propagation in a circumferential direction of a double layered poroelastic cylinder (consisting of a shaft-bearing assembly) is considered. The poroelastic materials of each shaft and bearing are assumed to be homogeneous and isotropic. The boundary condition at the interface [between the inner shaft and the bearing (outer hollow cylinder)] is assumed to be free-sliding; that is, the interfacial shear stresses are assumed to be zero, and the normal stress and radial displacements are continuous. The frequency equations are obtained for the model under consideration by using Biot's [10] theory of wave propagation. The frequency equation of a permeable and an impermeable surface for the cylindrical-piston assembly is obtained as a particular case of the model under consideration when the outer radius of the hollow poroelastic cylinder tends to infinity. When the angular wave number vanishes, the dilatational and shear waves are uncoupled in both the models and the frequency equation of shear waves is independent of the nature of the surface, that is, it is same for permeable and impermeable surfaces. Numerical results for the dispersion curves of the first three modes are presented and discussed.

2. Governing equations

The equations of motion of a homogeneous, isotropic poroelastic solid (Biot [10]) in the presence of dissipation *b* are

$$N\nabla^2 \boldsymbol{u} + (A+N)\nabla e + Q\nabla \in = \frac{\partial^2}{\partial t^2}\left(\rho_{11}\boldsymbol{u} + \rho_{12}\boldsymbol{U}\right) + b\frac{\partial}{\partial t}\left(\boldsymbol{u} - \boldsymbol{U}\right),$$

(2.1)

$$Q\nabla e + R\nabla \in = \frac{\partial^2}{\partial t^2}\left(\rho_{12}\boldsymbol{u} + \rho_{22}\boldsymbol{U}\right) - b\frac{\partial}{\partial t}\left(\boldsymbol{u} - \boldsymbol{U}\right)$$

where ∇^2 is the Laplacian, $\boldsymbol{u}\left(u_r, u_\theta, u_z\right)$ and $\boldsymbol{U}\left(U_r, U_\theta, U_z\right)$ are displacements of the solid and liquid respectively, e and $\in$ are the dilatations of solid and liquid; A, N, Q, R are poroelastic constants and $\rho_{jk}(j, k = 1, 2)$ are the mass coefficients following Biot [10]. The poroelastic constants A, N correspond to familiar Lame constants in a purely elastic solid. The coefficient N represents the shear modulus of the solid. The coefficient R is a measure of the pressure required on the liquid to force a certain amount of the liquid into the aggregate while the total volume remains constant. The coefficient Q represents the coupling between the volume change of the solid to that of the liquid.

For the present problem, we consider the displacement components of solid $\boldsymbol{u}\left(u_r, u_\theta, 0\right)$ and liquid $\boldsymbol{U}\left(U_r, U_\theta, 0\right)$

$$u_r = \frac{\partial \Phi_1}{\partial r} + \frac{1}{r}\frac{\partial \Psi_1}{\partial \theta}, \qquad u_\theta = \frac{1}{r}\frac{\partial \Phi_1}{\partial \theta} - \frac{\partial \Psi_1}{\partial r},$$

(2.2)

$$U_r = \frac{\partial \Phi_2}{\partial r} + \frac{1}{r}\frac{\partial \Psi_2}{\partial \theta}, \qquad U_\theta = \frac{1}{r}\frac{\partial \Phi_2}{\partial \theta} - \frac{\partial \Psi_2}{\partial r}$$

where Φ_1, Φ_2, ψ_1, ψ_2 are functions of r, θ and time t.
Substitution of Eq.(2.2) into Eq.(2.1) yields

$$P\nabla^2\Phi_1 + Q\nabla^2\Phi_2 = \frac{\partial^2}{\partial t^2}\left(\rho_{11}\Phi_1 + \rho_{12}\Phi_2\right) + b\frac{\partial}{\partial t}\left(\Phi_1 - \Phi_2\right),$$

$$Q\nabla^2\Phi_1 + R\nabla^2\Phi_2 = \frac{\partial^2}{\partial t^2}\left(\rho_{12}\Phi_1 + \rho_{22}\Phi_2\right) - b\frac{\partial}{\partial t}\left(\Phi_1 - \Phi_2\right),$$

(2.3)

$$N\nabla^2\Psi_1 = \frac{\partial^2}{\partial t^2}\left(\rho_{11}\Psi_1 + \rho_{12}\Psi_2\right) + b\frac{\partial}{\partial t}\left(\Psi_1 - \Psi_2\right),$$

$$0 = \frac{\partial^2}{\partial t^2}\left(\rho_{12}\Psi_1 + \rho_{22}\Psi_2\right) - b\frac{\partial}{\partial t}\left(\Psi_1 - \Psi_2\right)$$

where $P=A+2N$ and $\nabla^2 = \frac{\partial^2}{\partial r^2} + \frac{1}{r}\frac{\partial}{\partial r} + \frac{1}{r^2}\frac{\partial^2}{\partial \theta^2}$.

The stresses σ_{jk} and the liquid pressure s of the poroelastic solid are

$$\sigma_{jk} = 2Ne_{jk} + (Ae + Q\in)\delta_{jk}, \qquad \left(j, k = r, \theta, z\right),$$

(2.4)

$$s = Qe + R\in$$

where δ_{jk} is the well-known Kronecker delta function.

3. Solution of the problem

We consider a two layered poroelastic cylinder of infinite extent in the axial direction whose cross section is shown in Fig.1, where the axis of the cylinder is along the z-axis and (r, θ, z) are the cylindrical polar co-ordinates. Each layer of the poroelastic cylinder is isotropic and homogeneous. The radius of the inner shaft is r_1 and outer radius of the bearing (hollow cylinder) is r_2. For waves propagating in the circumferential direction the assumption of plane-strain deformation prevails. In this case, the pertinent non-zero displacement and stress components are $u_r, u_\theta, \sigma_{rr}, \sigma_{\theta\theta}, \sigma_{r\theta}$ and these are the variables of r and θ only. The physical parameters related to the inner shaft are denoted by * as a superscript. For example, poroelastic constants of the poroelastic outer cylinder (bearing) are A, N, Q, R and the poroelastic constants of the inner shaft are denoted by A^*, N^*, Q^*, R^*. We seek the solution of Eqs (2.3) in the form

$$\Phi_1 = F_1(r)e^{i(n\theta-\omega t)}, \qquad \Phi_2 = F_2(r)e^{i(n\theta-\omega t)},$$

$$\Psi_1 = G_1(r)e^{i(n\theta-\omega t)}, \qquad \Psi_2 = G_2(r)e^{i(n\theta-\omega t)}$$

$$(3.1)$$

where n is the angular wave number ω is the circular frequency and i is the complex unity. Equation (3.1) represents the potentials functions for time harmonic guided waves propagating in the circumferential direction and it is a model proposed by Viktorov [11] and then subsequently used by other authors. By substituting Eqs (3.1) into Eqs (2.3), its solution (bounded solution for the inner shaft) yields

$$F_1 = \begin{cases} \left[C_1 J_n(\xi_1 r) + C_2 Y_n(\xi_1 r) + C_3 J_n(\xi_2 r) + C_4 Y_n(\xi_2 r) \right], & r_1 < r < r_2, \\ \\ \left[D_1 J_n(\xi_1 r) + D_2 J_n(\xi_2 r) \right], & 0 < r < r_1, \end{cases} \quad \dots (3.2)$$

$$F_2 = \begin{cases} -\left[C_1 \delta_1^2 J_n(\xi_1 r) + C_2 \delta_1^2 Y_n(\xi_1 r) + C_3 \delta_2^2 J_n(\xi_2 r) + C_4 \delta_2^2 Y_n(\xi_2 r) \right], & r_1 < r < r_2, \\ \\ -[D_1 \delta_1^2 J_n(\xi_1 r) + D_2 \delta_2^2 J_n(\xi_2 r)], & 0 < r < r_1, \end{cases} \quad (3.3)$$

$$G_1 = \begin{cases} \left[C_5 J_n(\xi_3 r) + C_6 Y_n(\xi_3 r) \right], & r_1 < r < r_2, \\ \\ \left[D_3 J_n(\xi_3 r) \right], & 0 < r < r_1, \end{cases} \quad \dots (3.4)$$

$$G_2 = -K_{12}K_{22}^{-1} \begin{cases} \left[C_5 J_n(\xi_3 r) + C_6 Y_n(\xi_3 r) \right], & r_1 < r < r_2, \\ \\ \left[D_3 J_n(\xi_3 r) \right], & 0 < r < r_1. \end{cases} \quad \dots (3.5)$$

In Eqs (3.2), (3.3), (3.4), (3.5), $C_1, C_2, C_3, C_4, C_5, C_6, D_1, D_2, D_3$ are arbitrary constants, J_n and Y_n are Bessel functions of first and second kind each of order n and

$$\xi_j = \frac{\omega}{V_j}, \quad (j = 1, 2, 3), \qquad \delta_j^2 = \frac{\left[(RK_{11} - QK_{12}) - V_j^{-2}(PR - Q^2) \right]}{(RK_{12} - QK_{22})}, \quad (j = 1, 2). \quad (3.6)$$

In Eqs (3.6), V_1 and V_2 are the velocities of dilatational waves of first and second kind respectively, V_3 is the shear wave velocity and

$$K_{11} = \rho_{11} - \frac{ib}{\omega}, \qquad K_{12} = \rho_{12} + \frac{ib}{\omega}, \qquad K_{22} = \rho_{22} - \frac{ib}{\omega}. \qquad \ldots\text{(3.7)}$$

Employing Eqs (3.2), (3.3), (3.4), (3.5) into Eqs (3.1) and then using Eqs (2.2) we get the displacement components of the solid as

$$u_r = \begin{cases} \left\{ \left[C_1 \xi_1 J_n'\left(\xi_1 r\right) + C_2 \xi_1 Y_n'\left(\xi_1 r\right) + C_3 \xi_2 J_n'\left(\xi_2 r\right) + C_4 \xi_2 Y_n'\left(\xi_2 r\right) \right] + \\ + \dfrac{in}{r}\left[C_5 J_n\left(\xi_3 r\right) + C_6 Y_n\left(\xi_3 r\right) \right] \right\} e^{i(n\theta - \omega t)}, \qquad r_1 < r < r_2, \\[4mm] \left\{ D_1 \xi_1^* J_n'\left(\xi_1^* r\right) + D_2 \xi_2^* J_n'\left(\xi_2^* r\right) + D_3 \dfrac{in}{r} J_n\left(\xi_3^* r\right) \right\} e^{i(n\theta - \omega t)}, \qquad 0 < r < r_1, \end{cases}$$

(3.8)

$$u_\theta = \begin{cases} \left\{ \dfrac{in}{r}\left[C_1 J_n\left(\xi_1 r\right) + C_2 Y_n\left(\xi_1 r\right) + C_3 J_n\left(\xi_2 r\right) + C_4 Y_n\left(\xi_2 r\right) \right] + \\ -\xi_3 \left[C_5 J_n'\left(\xi_3 r\right) + C_6 \xi_3 Y_n'\left(\xi_3 r\right) \right] \right\} e^{i(n\theta - \omega t)}, \qquad r_1 < r < r_2, \\[4mm] \left\{ \dfrac{in}{r}\left[D_1 J_n\left(\xi_1^* r\right) + D_2 J_n\left(\xi_2^* r\right) \right] - D_3 \xi_3^* J_n'\left(\xi_3^* r\right) \right\} e^{i(n\theta - \omega t)}, \qquad 0 < r < r_1, \end{cases}$$

where a dash (/) over a quantity represents the differentiation with respect to r.

The non-zero stresses and liquid pressure in terms of potential functions are

$$\sigma_{rr} = 2N\left(\frac{\partial^2 \Phi_1}{\partial r^2} - \frac{1}{r^2}\frac{\partial \Psi_1}{\partial \theta} + \frac{1}{r}\frac{\partial^2 \Psi_1}{\partial \theta \partial r} \right) + A\nabla^2 \Phi_1 + Q\nabla^2 \Phi_2,$$

$$\sigma_{r\theta} = N\left(\frac{2}{r}\frac{\partial^2 \Phi_1}{\partial r \partial \theta} - \frac{2}{r^2}\frac{\partial \Phi_1}{\partial \theta} - \frac{\partial^2 \Psi_1}{\partial r^2} + \frac{1}{r^2}\frac{\partial^2 \Psi_1}{\partial \theta^2} + \frac{1}{r}\frac{\partial \Psi_1}{\partial r} \right), \qquad \text{(3.9)}$$

$$s = Q\nabla^2 \Phi_1 + R\nabla^2 \Phi_2$$

where

$$\nabla^2 = \frac{\partial^2}{\partial r^2} + \frac{1}{r}\frac{\partial}{\partial r} + \frac{1}{r^2}\frac{\partial^2}{\partial \theta^2}.$$

4. Boundary conditions – frequency equation

The outer surface of the cylinder (bearing) is assumed to be stress free and at the interface, the inner shaft and the outer cylinder (bearing) is free-sliding. Thus the boundary conditions for free vibrations in the case of a permeable surface are

$$\left(\sigma_{rr}+s\right)_{r=r_1^+}-\left(\sigma_{rr}^*+s^*\right)_{r=r_1^-}=0, \qquad \left(\sigma_{r\theta}\right)_{r=r_1^+}=0, \qquad \left(\sigma_{r\theta}^*\right)_{r=r_1^-}=0,$$

$$\left(u_r\right)_{r=r_1^+}-\left(u_r^*\right)_{r=r_1^-}=0, \qquad\qquad \left(s\right)_{r=r_1^+}=0, \qquad \left(s^*\right)_{r=r_1^-}=0, \qquad (4.1)$$

$$\sigma_{rr}+s=0, \qquad \sigma_{r\theta}=0, \qquad s=0, \qquad \text{at} \qquad r=r_2.$$

Similarly, the boundary conditions in the case of an impermeable surface are

$$\left(\sigma_{rr}+s\right)_{r=r_1^+}-\left(\sigma_{rr}^*+s^*\right)_{r=r_1^-}=0, \qquad \left(\sigma_{r\theta}\right)_{r=r_1^+}=0, \qquad \left(\sigma_{r\theta}^*\right)_{r=r_1^-}=0,$$

$$\left(u_r\right)_{r=r_1^+}-\left(u_r^*\right)_{r=r_1^-}=0, \qquad \left(\frac{\partial s}{\partial r}\right)_{r=r_1^+}=0, \qquad \left(\frac{\partial s^*}{\partial r}\right)_{r=r_1^-}=0, \qquad (4.2)$$

$$\sigma_{rr}+s=0, \qquad \sigma_{r\theta}=0, \qquad \frac{\partial s}{\partial r}=0, \qquad \text{at} \qquad r=r_2.$$

Putting Eqs (2.4), (3.8) and (3.9) into Eqs (4.1) results in a system of nine homogeneous algebraic equations of nine constants C_1, C_2, C_3, C_4, C_5, C_6, D_1, D_2, and D_3. For a non-trivial solution to exist, the determinant of the coefficients must vanish. By eliminating these constants, the frequency equation of guided circumferential waves of a layered poroelastic cylinder in the case of a permeable surface is

$$\left|M_{jk}\right|=0, \qquad j,k=1,2,3....9 \qquad (4.3)$$

where the elements $M_{jk}(r)$ are given in the Appendix [see Eq.(A.1)].

Arguing similarly, putting Eqs (2.4), (3.8) and (3.9) into Eqs (4.2) yields the frequency equation of guided circumferential waves of a layered poroelastic cylinder in the case of an impermeable surface to be

$$\left|N_{jk}\right|=0, \qquad j,k=1,2,3....9 \qquad (4.4)$$

where the elements $N_{jk}(r)$ are given in the Appendix [see Eq.(A.2)].

By eliminating liquid effects from the frequency equation of a permeable surface (4.3), that is, setting $b\to0$, $\rho_{12}\to0$, $\rho_{22}\to0$, $(A-Q^2/R)\to\lambda$, $N\to\mu$, $Q\to0$, $R\to0$ and after rearrangement of the terms, the results for a purely elastic solid are obtained as a particular case considered by Christine Valle et al. [2]. The frequency equation of an impermeable surface (4.4) has no counterpart in the purely elastic solid.

Now we consider two particular cases of the general frequency Eqs (4.3) and (4.4) of guided circumferential waves: (i) When the angular wave number vanishes. (ii) When the outer radius of the hollow poroelastic cylinder tends to infinity, the model under consideration (shaft-bearing assembly) reduces to the cylinder-piston assembly.

(i)   When the angular wave number n vanish, the frequency equation of a permeable surface that is Eqs (4.3) degenerates into the product

$$M_{39}\left(r_1\right)D_1D_2=0 \qquad (4.5)$$

where $M_{jk}(r)$ are defined in the Appendix [see Eq.(A.1)] and D_1, D_2 are

$$D_1 = \begin{vmatrix} M_{25}(r_1) & M_{26}(r_1) \\ M_{85}(r_2) & M_{85}(r_2) \end{vmatrix},$$

(4.6)

$$D_2 = \begin{vmatrix} M_{11}(r_1) & M_{12}(r_1) & M_{13}(r_1) & M_{14}(r_1) & M_{17}(r_1) & M_{18}(r_1) \\ M_{41}(r_1) & M_{42}(r_1) & M_{43}(r_1) & M_{44}(r_1) & M_{47}(r_1) & M_{48}(r_1) \\ M_{51}(r_1) & M_{52}(r_1) & M_{53}(r_1) & M_{54}(r_1) & 0 & 0 \\ 0 & 0 & 0 & 0 & M_{67}(r_1) & M_{68}(r_1) \\ M_{71}(r_2) & M_{72}(r_2) & M_{73}(r_2) & M_{74}(r_2) & 0 & 0 \\ M_{91}(r_2) & M_{92}(r_2) & M_{93}(r_2) & M_{94}(r_2) & 0 & 0 \end{vmatrix}.$$

Similarly, when the wave number n vanishes, the frequency equation of an impermeable surface [Eq.(4.4)] degenerates into the product

$$N_{39}(r_1) D_3 D_4 = 0$$

(4.7)

where $N_{jk}(r)$ are defined in the appendix [see Eq.(A.2)] and D_3, D_4 are

$$D_3 = \begin{vmatrix} N_{25}(r_1) & N_{26}(r_1) \\ N_{85}(r_2) & N_{85}(r_2) \end{vmatrix},$$

(4.8)

$$D_4 = \begin{vmatrix} N_{11}(r_1) & N_{12}(r_1) & N_{13}(r_1) & N_{14}(r_1) & N_{17}(r_1) & N_{18}(r_1) \\ N_{41}(r_1) & N_{42}(r_1) & N_{43}(r_1) & N_{44}(r_1) & N_{47}(r_1) & N_{48}(r_1) \\ N_{51}(r_1) & N_{52}(r_1) & N_{53}(r_1) & N_{54}(r_1) & 0 & 0 \\ 0 & 0 & 0 & 0 & N_{67}(r_1) & N_{68}(r_1) \\ N_{71}(r_2) & N_{72}(r_2) & N_{73}(r_2) & N_{74}(r_2) & 0 & 0 \\ N_{91}(r_2) & N_{92}(r_2) & N_{93}(r_2) & N_{94}(r_2) & 0 & 0 \end{vmatrix}.$$

Equation (4.5) is satisfied if, $M_{39}(r_1)=0$, or $D_1=0$ or $D_2=0$. Equation $M_{39}(r_1)=0$, when simplified reduces to $J_2\left(\xi_3^* r_1\right)=0$, which is similar to the frequency equation of torsional vibrations discussed by Tajuddin and Sarma [12]. The equation $D_1=0$, when simplified reduces to $J_2(\xi_3 r_1)Y_2(\xi_3 r_2) - J_2(\xi_3 r_2)Y_2(\xi_3 r_1) = 0$ which is the frequency equation of axially symmetric shear vibrations discussed by Malla Reddy and Tajuddin [7] and also similar to the frequency equation of torsional vibrations of hollow poroelastic cylinders discussed by Tajuddin and Ahmed Shah [4]. The equation

$$D_2=0,$$

(4.9)

 is the frequency equation of dilatational guided circumferential waves of the shaft-bearing assembly in the case of a permeable surface. From Eq.(4.5) we see that the dilatational and shear waves are uncoupled. It is important to note that the shear waves are uncoupled in the outer poroelastic cylinder (bearing) and the inner shaft. But the dilatational waves are coupled in shaft-bearing assembly. As discussed in the case of a permeable surface, from Eq.(4.7) we see that the frequency equation of dilatational circumferential waves for an impermeable surface is

$$D_4=0,$$

(4.10)

also it can be noted that the frequency equation of shear vibrations is independent of nature of surface, that is, it is same for a permeable and an impermeable surface.

(ii) When the outer radius of the outer poroelastic hollow cylinder (bearing) tends to infinity, the shaft-bearing model reduces to the cylinder-piston assembly. Analogous displacements and stresses for a circular cylindrical cavity in an infinite porous medium are written replacing Bessel functions of first and second kind by Bessel function of third kind (Hankel function), $H_n^{(1)}$ and $H_n^{(2)}$. Hankel functions may be expressed in the form of Bessel functions of first and second kind

$$H_n^{(1)} = J_n + iY_n, \qquad H_n^{(2)} = J_n - iY_n.$$

The Hankel function tends to zero as the argument becomes large, although the individual functions do not. For all values of n, the Hankel functions $H_n^{(1)}$ and $H_n^{(2)}$ are linearly independent. $H_n^{(1)}$ represents waves propagating towards the origin while $H_n^{(2)}$ represents waves diverging from the origin. Since there is no outer boundary, the terms containing $H_n^{(1)}$ must vanish. The displacement and stresses may then be written in terms of $H_n^{(2)}$. We see that after necessary calculations, $H_n^{(2)}$ is to be transformed to the Bessel function of second kind Y_n. Then the frequency equation of guided circumferential waves for the cylinder-piston assembly in the case of a permeable surface is

$$\begin{vmatrix} M_{12}(r_1) & M_{14}(r_1) & M_{16}(r_1) & M_{17}(r_1) & M_{18}(r_1) & M_{19}(r_1) \\ M_{22}(r_1) & M_{24}(r_1) & M_{26}(r_1) & 0 & 0 & 0 \\ 0 & 0 & 0 & M_{37}(r_1) & M_{38}(r_1) & M_{39}(r_1) \\ M_{42}(r_1) & M_{44}(r_1) & M_{46}(r_1) & M_{47}(r_1) & M_{48}(r_1) & M_{49}(r_1) \\ M_{52}(r_1) & M_{54}(r_1) & 0 & 0 & 0 & 0 \\ 0 & 0 & 0 & M_{67}(r_1) & M_{68}(r_1) & 0 \end{vmatrix} = 0 \,. \tag{4.11}$$

Similarly, the frequency equation of guided circumferential waves for the cylinder-piston assembly in the case of an impermeable surface is

$$\begin{vmatrix} N_{12}(r_1) & N_{14}(r_1) & N_{16}(r_1) & N_{17}(r_1) & N_{18}(r_1) & N_{19}(r_1) \\ N_{22}(r_1) & N_{24}(r_1) & N_{26}(r_1) & 0 & 0 & 0 \\ 0 & 0 & 0 & N_{37}(r_1) & N_{38}(r_1) & N_{39}(r_1) \\ N_{42}(r_1) & N_{44}(r_1) & N_{46}(r_1) & N_{47}(r_1) & N_{48}(r_1) & N_{49}(r_1) \\ N_{52}(r_1) & N_{54}(r_1) & 0 & 0 & 0 & 0 \\ 0 & 0 & 0 & N_{67}(r_1) & N_{68}(r_1) & 0 \end{vmatrix} = 0. \tag{4.12}$$

In Eqs (4.11) and (4.12), the elements $M_{jk}(r)$ and $N_{jk}(r)$ are defined in Eqs (A.1) and (A.2), respectively, in the appendix. Frequency Eqs (4.11) and (4.12) can be considered for zero angular wave number.

For further analysis of frequency Eqs (4.3) and (4.4), now we denote these equations by Δ_1 and Δ_2, respectively. After necessary simplifications, Eq.(4.3) can be re-written as

$$|\Delta_1| = \begin{vmatrix} \Delta_{11} & \Delta_{12} \\ \Delta_{21} & \Delta_{22} \end{vmatrix} = 0 \tag{4.13}$$

where the sub-determinants Δ_{jk} $(j, k=1, 2)$ are

$$\Delta_{11} = \begin{vmatrix} M_{37}(r_1) & M_{38}(r_1) & M_{39}(r_1) \\ M_{47}(r_1) & M_{48}(r_1) & M_{49}(r_1) \\ M_{67}(r_1) & M_{68}(r_1) & 0 \end{vmatrix}, \qquad \Delta_{12} = \begin{vmatrix} M_{17}(r_1) & M_{18}(r_1) & M_{19}(r_1) \\ M_{37}(r_1) & M_{38}(r_1) & M_{39}(r_1) \\ M_{67}(r_1) & M_{68}(r_1) & 0 \end{vmatrix},$$

$$\Delta_{21} = \begin{vmatrix} M_{21}(r_1) & M_{22}(r_1) & M_{23}(r_1) & M_{24}(r_1) & M_{25}(r_1) & M_{26}(r_1) \\ M_{41}(r_1) & M_{42}(r_1) & M_{43}(r_1) & M_{44}(r_1) & M_{45}(r_1) & M_{46}(r_1) \\ M_{51}(r_1) & M_{52}(r_1) & M_{53}(r_1) & M_{54}(r_1) & 0 & 0 \\ M_{71}(r_2) & M_{72}(r_2) & M_{73}(r_2) & M_{74}(r_2) & M_{75}(r_2) & M_{76}(r_2) \\ M_{81}(r_2) & M_{82}(r_2) & M_{83}(r_2) & M_{84}(r_2) & M_{85}(r_2) & M_{86}(r_2) \\ M_{91}(r_2) & M_{92}(r_2) & M_{93}(r_2) & M_{94}(r_2) & 0 & 0 \end{vmatrix}, \qquad (4.14)$$

$$\Delta_{22} = \begin{vmatrix} M_{11}(r_1) & M_{12}(r_1) & M_{13}(r_1) & M_{14}(r_1) & M_{15}(r_1) & M_{16}(r_1) \\ M_{21}(r_1) & M_{22}(r_1) & M_{23}(r_1) & M_{24}(r_1) & M_{25}(r_1) & M_{26}(r_1) \\ M_{51}(r_1) & M_{52}(r_1) & M_{53}(r_1) & M_{54}(r_1) & 0 & 0 \\ M_{71}(r_2) & M_{72}(r_2) & M_{73}(r_2) & M_{74}(r_2) & M_{75}(r_2) & M_{76}(r_2) \\ M_{81}(r_2) & M_{82}(r_2) & M_{83}(r_2) & M_{84}(r_2) & M_{85}(r_2) & M_{86}(r_2) \\ M_{91}(r_2) & M_{92}(r_2) & M_{93}(r_2) & M_{94}(r_2) & 0 & 0 \end{vmatrix}$$

where the elements $M_{jk}(r)$ are defined in the appendix [see Eq.(A.1)]. If the determinant $|\Delta_{22}|$ is singular, then it represents the frequency equation of guided circumferential waves in the hollow poroelastic cylinder for a permeable surface. This equation is similar (not same) to the frequency equation of plane-strain vibrations studied by Malla Reddy and Tajuddin [7] for a permeable surface. Then Eq.(4.13) reduces to $|\Delta_{12}| = 0$ which represents the frequency equation of guided circumferential waves in a poroelastic solid cylinder of radius r_1 for a permeable surface. Similarly, the frequency equation of an impermeable surface (4.4) can be simplified in the form

$$|\Delta_2| = \begin{vmatrix} \Delta_{11}^* & \Delta_{12}^* \\ \Delta_{21}^* & \Delta_{22}^* \end{vmatrix} = 0 \qquad (4.15)$$

where the sub-determinants Δ_{jk}^* (j, $k=1$, 2) are exactly same as the sub-determinants defined in Eqs (4.14) with $M_{jk}(r)$ replaced by $N_{jk}(r)$, where $N_{jk}(r)$ are defined in the appendix [see Eq.(A.2)]. Analysis of Eq.(4.15), that is the frequency equation of an impermeable surface, is the same as that of the analysis of Eq.(4.13) described above.

5. Non-dimensionalisation of frequency equation

The wave number is real for propagating modes in a non-dissipative medium. The non-dimensional frequency Ω ($\omega h/C_0^*$) as a function of the non-dimensional angular wave number is computed for two types of shaft-bearing models and the cylinder-piston models. The geometric parameter for the model under consideration is $g=r_2/r_1$. To analyze the frequency equations of permeable and impermeable surfaces, it is convenient to introduce the following non-dimensional parameters

$$a_1 = PH^{*-1}, \quad a_2 = QH^{*-1}, \quad a_3 = RH^{*-1}, \quad a_4 = NH^{*-1},$$

$$m_{11} = \rho_{11}\rho^{*-1}, \quad m_{12} = \rho_{12}\rho^{*-1}, \quad m_{22} = \rho_{22}\rho^{*-1},$$

$$b_1 = P^*H^{*-1}, \quad b_2 = Q^*H^{*-1}, \quad b_3 = R^*H^{*-1}, \quad b_4 = N^*H^{*-1},$$

$$n_{11} = \rho_{11}^*\rho^{*-1}, \quad n_{12} = \rho_{12}^*\rho^{*-1}, \quad n_{22} = \rho_{22}^*\rho^{*-1},$$

(5.1)

$$x_1 = \left(V_0^* \; V_1^{-1}\right)^2, \quad y_1 = \left(V_0^* \; V_2^{-1}\right)^2, \quad z_1 = \left(V_0^* \; V_3^{-1}\right)^2, \quad x_1^* = \left(V_0^* \; V_1^{*-1}\right)^2,$$

$$y_1^* = \left(V_0^* \; V_2^{*-1}\right)^2, \quad z_1^* = \left(V_0^* \; V_3^{*-1}\right)^2$$

where $H^* = P^* + 2Q^* + R^*$, $\rho^* = \rho_{11}^* + 2\rho_{12}^* + \rho_{22}^*$. Also C_0^* and V_0^* are reference velocities ($C_0^{*2} = N^*/\rho^*$, $V_0^{*2} = H^*/\rho^*$). Frequency Eqs (4.3), (4.4), (4.11) and (4.12) are non-dimensionalised employing Eq.(5.1). These equations constitute a relation between the non-dimensional frequency and angular wave number.

Parameters of two types of shaft-bearing assembly models are considered designated as Model-I and Model-II to compute the non-dimensional frequency. Model-I consists of a shaft made of sandstone saturated with kerosene (Fatt [13]) and the bearing made of sandstone saturated with water (Yew and Jogi [14]). Model-II consists of a shaft made of water saturated sandstone and a bearing made of kerosene saturated sandstone.

The non-dimensional physical parameters of Model-I and Model-II are given in Tab.1

Material Parameter	a_1	a_2	a_3	a_4	m_{11}	m_{12}	m_{22}	x_1	y_1	z_1
Model-I	0.445	0.034	0.015	0.123	0.887	-0.001	0.099	1.863	8.884	7.183
Model-II	1.819	0.011	0.054	0.780	0.891	0	0.125	0.489	2.330	1.142

b_1	b_2	b_3	b_4	n_{11}	n_{12}	n_{22}	x_1^*	y_1^*	z_1^*
0.960	0.006	0.028	0.412	0.877	0	0.123	0.913	4.347	2.129
0.843	0.065	0.028	0.234	0.901	-0.001	0.101	0.999	4.763	3.851

6. Numerical results and discussion

Since stress wave propagation is the phenomenon of energy transfer, it plays a major role in fretting. Thus for the analysis of frequency equations of guided circumferential waves, Eqs (4.3), (4.4), (4.11) and (4.12) are non-dimensionalised employing Eqs (5.1) for computational work. For a given poroelastic model, these frequency equations constitute a relation between the non-dimensional frequency and angular wave

number for fixed values of *g*. Different values of *g*, viz., *1.2362* and *5.0* are taken for numerical computation. The non-dimensional frequency is determined for different values of the angular wave number n and for fixed values of *g*, each for a permeable and an impermeable surface. The frequency of guided circumferential waves of first three modes of the shaft-bearing assembly for Model-I is presented in Fig.2 for a permeable and an impermeable surface. From the figure we see that waves are more dispersive in a permeable surface. The first two modes of an impermeable surface are almost linear. By increasing the thickness of the bearing, the frequency is obtained for Model-I and it is presented in Fig.3. Here we see that all the modes are linear when the wave number is more than 6, and before it they are more dispersive. The frequency of an impermeable surface is less than that of a permeable surface for first three modes. Also, in general, it is seen that the frequency is larger for Model-I with an increased thickness. Figures 4 and 5 show the frequency as a function of the wave number for Model-II for the shaft-bearing assembly. The variation of frequency in Figure.4 is similar to that in Fig.2 and in Fig.5 to that in Fig.3. The frequency of an impermeable surface is less than that of a permeable surface in this case also. The frequency is larger for Model-II than that of Model-I. The frequency of bore-piston assembly for Model-I is presented in Fig.6 for a permeable and an impermeable surface. From the figure it is seen that the frequency of an impermeable surface is more that of a permeable surface when the wave number is more than 6. And in this range, the frequency of a permeable surface is linear. This is in contrast with the shaft-bearing assembly. This is not the case for Model-II of the cylinder-piston assembly shown in Fig.7. Also, we see that the first mode of an impermeable surface is linear but not the other modes. Also, in general, the frequency for Model-II is more than that of Model-I. Also the frequency is obtained for the said Model-I and Model-II for a permeable and an impermeable surface for the shaft-bearing assembly and the cylinder-piston assembly for a small wave number in the interval [0, 1] and it is seen that the variation of frequency is similar as mentioned above.
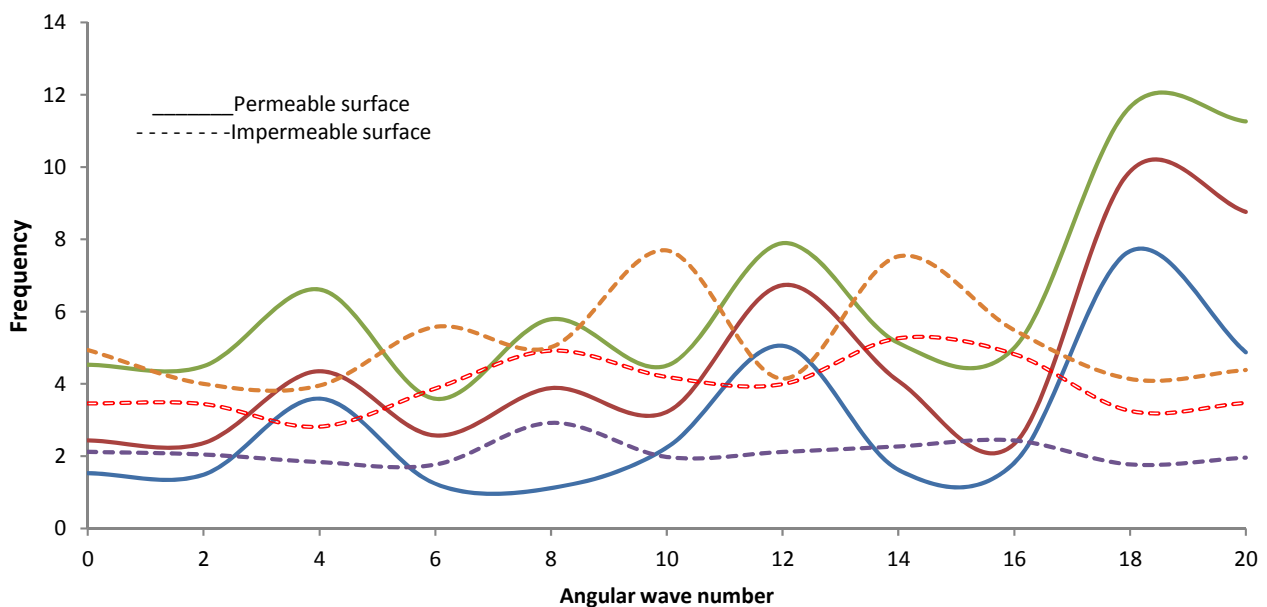

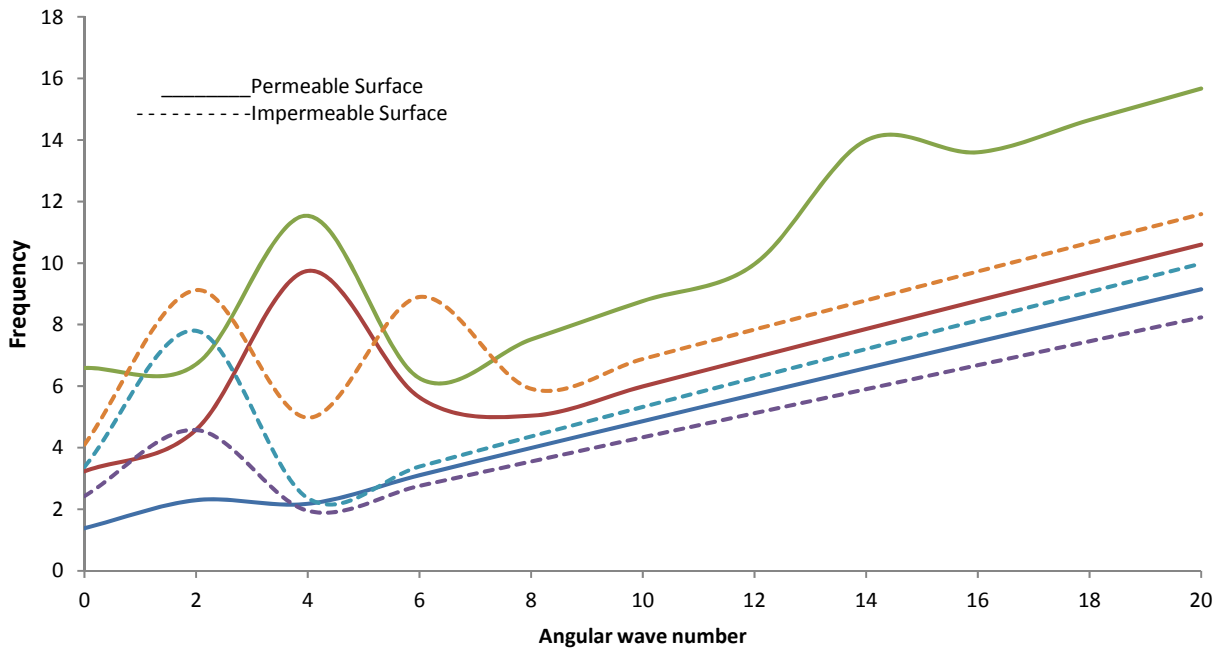Fig.2. Frequency as a function of wave number (shaft-bearing assembly, Model-I, *g=1.2362*).

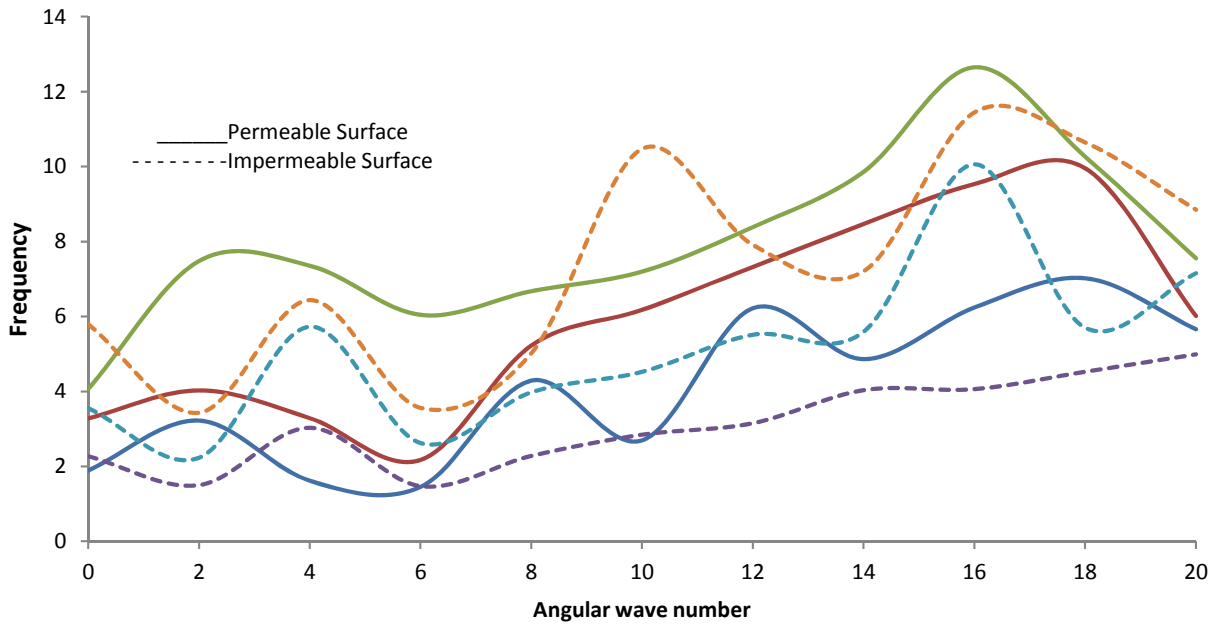Fig.3. Frequency as a function of wave number (shaft-bearing assembly, Model-I, *g=5*).

Fig.4. Frequency as a function of wave number (shaft-bearing assembly, Model-II, *g=1.2362*).
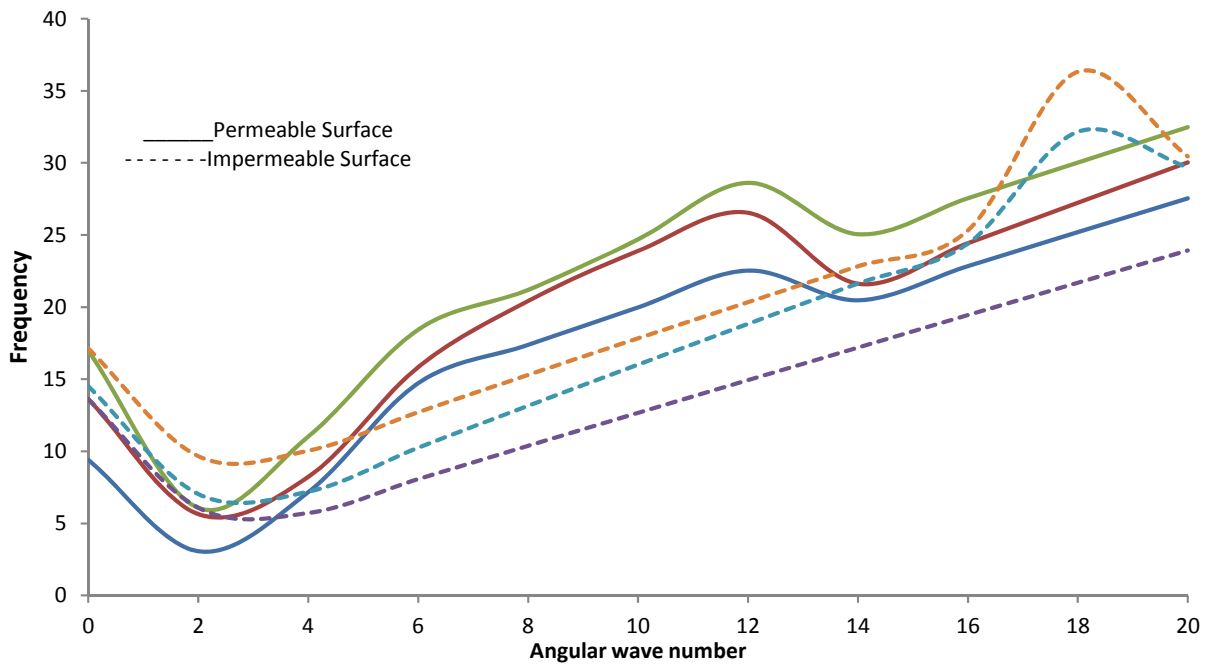
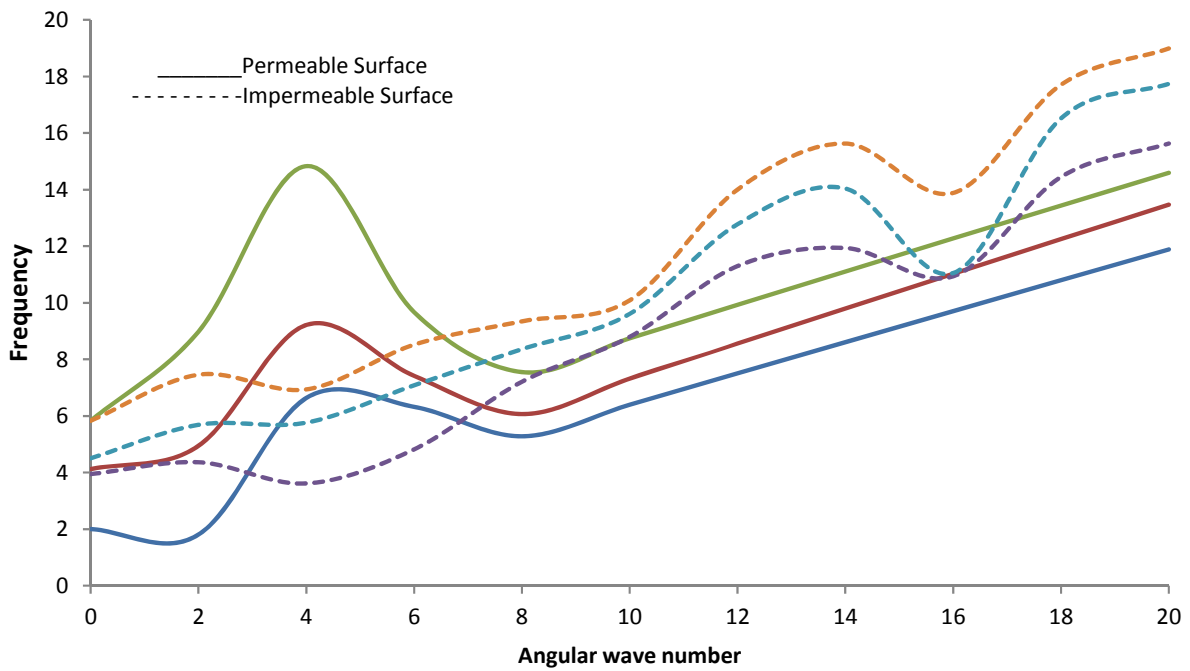Fig.5. Frequency as a function of wave number (shaft-bearing assembly, Model-II, *g=5*).

Fig.6. Frequency as a function of wave number (bore-piston assembly, Model-I).
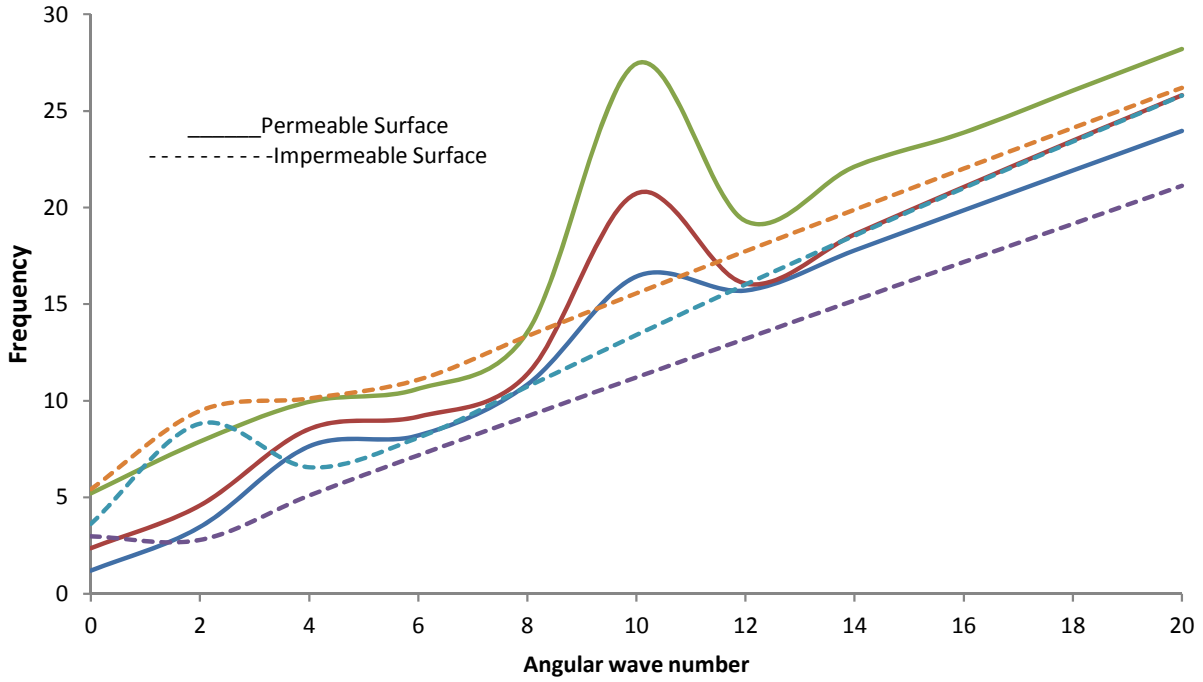
Fig.7. Frequency as a function of wave number (bore-piston assembly, Model-II).

7. Appendix

$$M_{11}(r_1) = -\frac{2N\xi_1}{r_1} J_n'(\xi_1 r_1) + \left\{ 2N\left(\frac{n^2}{r_1^2} - \xi_1^2\right) + \left[(Q+R)\delta_1^2 - (A+Q)\right]\xi_1^2 \right\} J_n(\xi_1 r_1),$$

$$M_{12}(r_1) = -\frac{2N\xi_1}{r_1} Y_n'(\xi_1 r_1) + \left\{ 2N\left(\frac{n^2}{r_1^2} - \xi_1^2\right) + \left[(Q+R)\delta_1^2 - (A+Q)\right]\xi_1^2 \right\} Y_n(\xi_1 r_1),$$

$$M_{13}(r_1) = -\frac{2N\xi_2}{r_1} J_n'(\xi_2 r_1) + \left\{ 2N\left(\frac{n^2}{r_1^2} - \xi_2^2\right) + \left[(Q+R)\delta_2^2 - (A+Q)\right]\xi_2^2 \right\} J_n(\xi_2 r_1),$$

$$M_{14}(r_1) = -\frac{2N\xi_2}{r_1} Y_n'(\xi_2 r_1) + \left\{ 2N\left(\frac{n^2}{r_1^2} - \xi_2^2\right) + \left[(Q+R)\delta_2^2 - (A+Q)\right]\xi_2^2 \right\} Y_n(\xi_2 r_1),$$

$$M_{15}(r_1) = -\frac{2Nin\xi_3}{r_1} J_n'(\xi_3 r_1) + \frac{2Nin}{r_1^2} J_n(\xi_3 r_1), \qquad M_{16}(r_1) = -\frac{2Nin\xi_3}{r_1} Y_n'(\xi_3 r_1) + \frac{2Nin}{r_1^2} Y_n(\xi_3 r_1),$$

$$M_{17}(r_1) = \frac{2N^*\xi_1^*}{r_1} J_n'(\xi_1^* r_1) - \left\{ 2N^*\left(\frac{n^2}{r_1^2} - \xi_1^{*2}\right) + \left[(Q^*+R^*)\delta_1^{*2} - (A^*+Q^*)\right]\xi_1^{*2} \right\} J_n(\xi_1^* r_1),$$

$$M_{18}(r_1) = \frac{2N^*\xi_2^*}{r_1} J_n'\left(\xi_2^* r_1\right) - \left\{ 2N^*\left(\frac{n^2}{r_1^2} - \xi_2^{*2}\right) + \left[\left(Q^* + R^*\right)\delta_2^{*2} - \left(A^* + Q^*\right)\right]\xi_2^{*2}\right\} J_n\left(\xi_2^* r_1\right),$$

$$M_{19}(r_1) = \frac{2N^* in\xi_3^*}{r_1} J_n'\left(\xi_3^* r_1\right) - \frac{2N^* in}{r_1^2} J_n\left(\xi_3^* r_1\right), \qquad M_{21}(r_1) = -\frac{2Nin\xi_1}{r_1} J_n'\left(\xi_1 r_1\right) - \frac{Nin}{r_1^2} J_n\left(\xi_1 r_1\right),$$

$$M_{22}(r_1) = -\frac{2Nin\xi_1}{r_1} Y_n'\left(\xi_1 r_1\right) - \frac{Nin}{r_1^2} Y_n\left(\xi_1 r_1\right), \qquad M_{23}(r_1) = -\frac{2Nin\xi_2}{r_1} J_n'\left(\xi_2 r_1\right) - \frac{Nin}{r_1^2} J_n\left(\xi_2 r_1\right),$$

$$M_{24}(r_1) = -\frac{2Nin\xi_2}{r_1} Y_n'\left(\xi_2 r_1\right) - \frac{Nin}{r_1^2} Y_n\left(\xi_2 r_1\right), \qquad M_{25}(r_1) = \frac{\xi_3}{r_1} J_n'\left(\xi_3 r_1\right) + \left(\xi_3^2 - \frac{2n^2}{r_1^2}\right) J_n\left(\xi_3 r_1\right),$$

$$M_{26}(r_1) = \frac{\xi_3}{r_1} Y_n'\left(\xi_3 r_1\right) + \left(\xi_3^2 - \frac{2n^2}{r_1^2}\right) Y_n\left(\xi_3 r_1\right),$$

$$M_{27}(r_1) = 0, \qquad M_{28}(r_1) = 0, \qquad M_{29}(r_1) = 0,$$

$$M_{31}(r_1) = 0, \quad M_{32}(r_1) = 0, \quad M_{33}(r_1) = 0, \quad M_{34}(r_1) = 0, \quad M_{35}(r_1) = 0, \quad M_{36}(r_1) = 0,$$

$$M_{37}(r_1) = -\frac{2N^* in\xi_1^*}{r_1} J_n'\left(\xi_1^* r_1\right) - \frac{N^* in}{r_1^2} J_n\left(\xi_1^* r_1\right), \qquad M_{38}(r_1) = -\frac{2N^* in\xi_2^*}{r_1} J_n'\left(\xi_2^* r_1\right) - \frac{N^* in}{r_1^2} J_n\left(\xi_2^* r_1\right),$$

$$M_{39}(r_1) = \frac{\xi_3^*}{r_1} J_n'\left(\xi_3^* r_1\right) + \left(\xi_3^{*2} - \frac{2n^2}{r_1^2}\right) J_n\left(\xi_3^* r_1\right),$$

$$M_{41}(r_1) = \xi_1 J_n'\left(\xi_1 r_1\right), \qquad M_{42}(r_1) = \xi_1 Y_n'\left(\xi_1 r_1\right), \qquad M_{43}(r_1) = \xi_2 J_n'\left(\xi_2 r_1\right),$$

$$M_{44}(r_1) = \xi_2 Y_n'\left(\xi_2 r_1\right), \qquad M_{45}(r_1) = \frac{in}{r_1} J_n\left(\xi_3 r_1\right), \qquad M_{46}(r_1) = \frac{in}{r_1} Y_n\left(\xi_3 r_1\right),$$

$$M_{47}(r_1) = -\xi_1^* J_n'\left(\xi_1^* r_1\right), \qquad M_{48}(r_1) = -\xi_2^* J_n'\left(\xi_2^* r_1\right), \qquad M_{49}(r_1) = -\frac{in}{r_1} J_n\left(\xi_3^* r_1\right),$$

$$M_{51}(r_1) = \left(R\delta_1^2 - Q\right)\xi_1^2 J_n\left(\xi_1 r_1\right), \qquad M_{52}(r_1) = \left(R\delta_1^2 - Q\right)\xi_1^2 Y_n\left(\xi_1 r_1\right),$$

$$M_{53}(r_1) = \left(R\delta_2^2 - Q\right)\xi_2^2 J_n\left(\xi_2 r_1\right), \qquad M_{54}(r_1) = \left(R\delta_2^2 - Q\right)\xi_2^2 Y_n\left(\xi_2 r_1\right),$$

$$M_{55}(r_1) = 0, \quad M_{56}(r_1) = 0, \quad M_{57}(r_1) = 0, \quad M_{58}(r_1) = 0, \quad M_{59}(r_1) = 0,$$

$$M_{61}(r_1)=0, \quad M_{62}(r_1)=0, \quad M_{63}(r_1)=0, \quad M_{64}(r_1)=0, \quad M_{65}(r_1)=0, \quad M_{66}(r_1)=0,$$

$$M_{67}(r_1)=\left(R^*\delta_1^{*2}-Q^*\right)\xi_1^{*2}J_n\left(\xi_1^* r_1\right), \qquad M_{68}(r_1)=\left(R^*\delta_2^{*2}-Q^*\right)\xi_2^{*2}J_n\left(\xi_2^* r_1\right), \qquad M_{69}(r_1)=0,$$

$$M_{71}(r_2)=-\frac{2N\xi_1}{r_2}J_n'(\xi_1 r_2)+\left\{2N\left(\frac{n^2}{r_2^2}-\xi_1^2\right)+\left[(Q+R)\delta_1^2-(A+Q)\right]\xi_1^2\right\}J_n(\xi_1 r_2),$$

$$M_{72}(r_2)=-\frac{2N\xi_1}{r_2}Y_n'(\xi_1 r_2)+\left\{2N\left(\frac{n^2}{r_2^2}-\xi_1^2\right)+\left[(Q+R)\delta_1^2-(A+Q)\right]\xi_1^2\right\}Y_n(\xi_1 r_2),$$

$$M_{73}(r_2)=-\frac{2N\xi_2}{r_2}J_n'(\xi_2 r_2)+\left\{2N\left(\frac{n^2}{r_2^2}-\xi_2^2\right)+\left[(Q+R)\delta_2^2-(A+Q)\right]\xi_2^2\right\}J_n(\xi_2 r_2),$$

$$M_{74}(r_2)=-\frac{2N\xi_2}{r_2}Y_n'(\xi_2 r_2)+\left\{2N\left(\frac{n^2}{r_2^2}-\xi_2^2\right)+\left[(Q+R)\delta_2^2-(A+Q)\right]\xi_2^2\right\}Y_n(\xi_2 r_2),$$

$$M_{75}(r_2)=-\frac{2Nin\xi_3}{r_2}J_n'(\xi_3 r_2)+\frac{2Nin}{r_2^2}J_n(\xi_3 r_2),$$

$$M_{76}(r_2)=-\frac{2Nin\xi_3}{r_2}Y_n'(\xi_3 r_2)+\frac{2Nin}{r_2^2}Y_n(\xi_3 r_2), \quad M_{77}(r_2)=0, \quad M_{78}(r_2)=0, \quad M_{79}(r_2)=0,$$

$$M_{81}(r_2)=-\frac{2Nin\xi_1}{r_2}J_n'(\xi_1 r_2)-\frac{Nin}{r_2^2}J_n(\xi_1 r_2) \qquad M_{82}(r_2)=-\frac{2Nin\xi_1}{r_2}Y_n'(\xi_1 r_2)-\frac{Nin}{r_2^2}Y_n(\xi_1 r_2),$$

$$M_{83}(r_2)=-\frac{2Nin\xi_2}{r_2}J_n'(\xi_2 r_2)-\frac{Nin}{r_2^2}J_n(\xi_2 r_2) \qquad M_{84}(r_2)=-\frac{2Nin\xi_2}{r_2}Y_n'(\xi_2 r_2)-\frac{Nin}{r_2^2}Y_n(\xi_2 r_2)$$

$$M_{85}(r_2)=\frac{\xi_3}{r_2}J_n'(\xi_2 r_2)+\left(\xi_3^2-\frac{2n^2}{r_2^2}\right)J_n(\xi_3 r_2) \qquad M_{86}(r_2)=\frac{\xi_3}{r_2}Y_n'(\xi_3 r_2)+\left(\xi_3^2-\frac{2n^2}{r_2^2}\right)Y_n(\xi_3 r_2)$$

$$M_{87}(r_2)=0, \qquad M_{88}(r_2)=0, \qquad M_{89}(r_2)=0,$$

$$M_{91}(r_2)=\left(R\delta_1^2-Q\right)\xi_1^2 J_n(\xi_1 r_2), \qquad M_{92}(r_2)=\left(R\delta_1^2-Q\right)\xi_1^2 Y_n(\xi_1 r_2),$$

$$M_{93}(r_2)=\left(R\delta_2^2-Q\right)\xi_2^2 J_n(\xi_2 r_2), \qquad M_{94}(r_2)=\left(R\delta_2^2-Q\right)\xi_2^2 Y_n(\xi_2 r_2),$$

$$M_{95}(r_2)=0, \quad M_{96}(r_2)=0, \quad M_{97}(r_2)=0, \quad M_{98}(r_2)=0, \quad M_{99}(r_2)=0. \qquad\qquad \text{…..(A.1)}$$

$$N_{jk}(r) = M_{jk}(r), \qquad j = 1, 2, 3, 4, 7, 8, \quad \text{and} \quad k = 1, 2, 3, 4, 5, 6, 7, 8, 9,$$

$$N_{51}(r_1) = \left(R\delta_1^2 - Q\right)\xi_1^3 J_n'(\xi_1 r_1), \qquad N_{52}(r_1) = \left(R\delta_1^2 - Q\right)\xi_1^3 Y_n'(\xi_1 r_1),$$

$$N_{53}(r_1) = \left(R\delta_2^2 - Q\right)\xi_2^3 J_n'(\xi_2 r_1), \qquad N_{54}(r_1) = \left(R\delta_2^2 - Q\right)\xi_2^3 Y_n'(\xi_2 r_1),$$

$$N_{55}(r_1) = 0, \quad N_{56}(r_1) = 0, \quad N_{57}(r_1) = 0, \quad N_{58}(r_1) = 0, \quad N_{59}(r_1) = 0,$$

$$N_{61}(r_1) = 0, \quad N_{62}(r_1) = 0, \quad N_{63}(r_1) = 0, \quad N_{64}(r_1) = 0, \quad N_{65}(r_1) = 0, \quad N_{66}(r_1) = 0,$$

$$N_{67}(r_1) = \left(R^*\delta_1^{*2} - Q^*\right)\xi_1^{*3} J_n'\left(\xi_1^* r_1\right), \qquad N_{68}(r_1) = \left(R^*\delta_2^{*2} - Q^*\right)\xi_2^{*3} J_n'\left(\xi_2^* r_1\right), \qquad M_{69}(r_1) = 0,$$

$$N_{91}(r_2) = \left(R\delta_1^2 - Q\right)\xi_1^3 J_n'(\xi_1 r_2), \qquad N_{92}(r_2) = \left(R\delta_1^2 - Q\right)\xi_1^3 Y_n'(\xi_1 r_2),$$

$$N_{93}(r_2) = \left(R\delta_2^2 - Q\right)\xi_2^3 J_n'(\xi_2 r_2), \qquad N_{94}(r_2) = \left(R\delta_2^2 - Q\right)\xi_2^3 Y_n'(\xi_2 r_2),$$

$$N_{95}(r_2) = 0, \quad N_{96}(r_2) = 0, \quad N_{97}(r_2) = 0, \quad N_{98}(r_2) = 0, \quad N_{99}(r_2) = 0. \qquad \dots\text{(A.2)}$$

Nomenclature

A, N, Q, R	− poroelastic constants of bearing
A^*, N^*, Q^*, R^*	− poroelastic constants of shaft
b	− dissipation
C_0^*, V_0^*	− reference velocities
g	− ratio of outer to inner radius
$H_n^{(1)}, H_n^{(2)}$	− Hankel function [Bessel function of third kind]
J_n, Y_n	− Bessel functions of first and second kind of order n
n	− angular wavenumber
(r, θ, z)	− cylindrical polar coordinates
r_2, r_1	− outer radius bearing, inner radius of shaft respectively
$U(U_r, U_\theta, 0)$	− displacement of liquid
$u(u_r, v_\theta, 0)$	− displacement of solid
V_1, V_2	− dilatational wave velocities of first and second kind respectively
V_3	− shear wave velocity
Ω	− non-dimensional frequency
ω	− circular frequency
∇^2	− Laplacian operator

References

[1] Nagy P.B., Blodgett M. and Godis M. (1994): *Weep hole inspection by circumferential creeping waves*. − NDT and E., vol.27, pp.131-142.

[2] Christine Valle, Jianmin Qu and Jacobs L.J. (1999): *Guided circumferential waves in layered cylinders*. − International Journal of Engineering Science, vol.37, pp.1369-1387.

[3] Tajuddin M. and Ahmed Shah S. (2006): *Circumferential waves of infinite hollow poroelastic cylinders*. − Trans. ASME, J. Appl. Mech., vol.73, pp.705-708.

[4] Tajuddin M. and Ahmed Shah S. (2007): *On torsional vibration of infinite hollow poroelastic cylinders*. − Journal of Mechanics of Materials and Structures, vol.2, pp.189-200.

[5] Whittier J.S. and Jones J.P. (1967): *Axially symmetric wave propagation in a two-layered cylinder*. − International Journal of Solids and Structures, vol.3, pp.657-675.

[6] Liu G. and Qu J. (1998): *Guided circumferential waves in a circular annulus*. − Trans. ASME, J. Appl. Mech., vol.65, pp.424-430.

[7] Malla Reddy P. and Tajuddin M. (2000): *Exact analysis of the plane-strain vibrations of thick-walled hollow poroelastic cylinders*. − International Journal of Solids and Structures, vol.37, pp.3439-3456.

[8] Towfighi S. Kundu T. and Ehsani M. (2002): *Elastic wave propagation in circumferential direction in anisotropic cylindrical curved plates*. − Trans. ASME. J. Appl. Mechanics, vol.69, pp.283-291.

[9] Ahmed Shah S. (2011): *Flexural wave propagation in coated poroelastic cylinders with reference to fretting fatigue*. − Journal of Vibration and Control, vol.17, pp.1049-1064.

[10] Biot M.A. (1956): *Theory of propagation of elastic waves in fluid-saturated porous solid*. − J. Acoust. Soc. Am., vol.28, pp.168-178.

[11] Viktorov I.A. (1958): *Rayleigh-type waves on curved surfaces*. − J. Acoust. Soc. Am, vol.4, pp.131-136.

[12] Tajuddin M. and Sarma K.S. (1980): *Torsional vibrations of poroelastic cylinders*. − Trans. ASME, J. Appl. Mech., vol.47, pp.214-216.

[13] Fatt I. (1959): *The Biot-Willis elastic coefficients for a sandstone*. − J. Appl. Mech., vol.26, pp.296-297.

[14] Yew C.H. and Jogi P.N. (1976): *Study of wave motions in fluid-saturated porous rocks*. − J. Acoust. Soc. Am, vol.60, pp.2-8.

[15] Abramowitz A. and Stegun I.A. (1965): *Handbook of Mathematical Functions*. − National Bureau of Standards, Washington, D.C.